Interaction of fluttering webs with surrounding air

Young B. Chang and Peter M. Moretti
Research associate and professor, respectively, Oklahoma State University, Engineering North 218, Stillwater, Okla. 74078-0545

ABSTRACT *The out-of-plane flutter of a moving web was studied, initially by analysis of the governing equation. The dynamic terms in the equation include transverse acceleration, Coriolis, and centrifugal forces. Each of the dynamic terms is affected differently by the air, depending on the air flow and the surrounding enclosure. A method for computing the effect of the surrounding enclosure on the aerodynamic inertia coefficient has been developed and is demonstrated in an example.*

Wind-tunnel experiments have been carried out to determine the influence of parallel air flow. Two different instabilities, steady deflection and flutter, have been detected. The results apply to the design and troubleshooting of paper machinery and printing presses, particularly with regard to the management of air flow for drying. In addition, the added-mass coefficients obtained can be used in implementing computer simulations of web dynamics.

KEYWORDS
Air flow
Analysis
Drying
Fluid dynamics
Papermaking
Runnability
Tension control
Web

As papermaking machines are pushed to higher speeds, the incidence and severity of out-of-plane vibrations (or flutter) increase, leading to quality problems and a higher probability of breaks. Generally, these breaks are blamed on a local weakness in the paper, but at least part of the cause is often flutter.

Vibration of the web leads to large intermittent stresses, especially at the edges of the web, or else the steady tension is kept too high to keep these oscillations under control. Unfortunately, it is difficult for the operator to know whether too much or too little tension is contributing to the incidence of web breaks. Therefore, analysis is needed (a) to find the best balance between excessive vibration and excessive tension, (b) to suggest modifications that will improve the runnability of a web line, and (c) to predict and increase the running speed of new installations.

Fluttering of a moving web is often analyzed by using the "threadline" model, in which the CD (cross-direction) variation of web motion is neglected by assuming that the entire width of the web deflects uniformly. Pramila studied this model (*1*), including aerodynamic terms, assuming that the web is in an infinite air space and all the surrounding air moves at the same speed as the web. Later, Pramila considered the possibility that the air may be stationary (*2*). In actuality, the air flow around the running web is very different from these two ideal cases: in the pockets of air on paper machines, the flow field is much more complicated (*3-5*).

If we do a force balance on an infinitesimal element of area of a traveling web or sheet, we obtain the complicated partial differential equation:

See Equation 1

where

x = position in the machine direction

y = position in the cross-machine direction

z = out-of-plane deflection

v = web velocity in the machine direction

t = time

D = bending stiffness of sheet

T = tension per unit width in the web

m = mass per unit area of the web material

m_1 = added mass associated with transverse acceleration

m_2 = added mass associated with Coriolis acceleration

m_3 = added mass associated with centripetal acceleration.

Equations:

$$f(x,y,t) = (m + m_1)\frac{\partial^2 z}{\partial t^2} + 2(m + m_2)v\frac{\partial^2 z}{\partial t \partial x} + (m + m_3)v^2\frac{\partial^2 z}{\partial x^2} - T\frac{\partial^2 z}{\partial x^2} + D\left(\frac{\partial^2}{\partial x^2} + \frac{\partial^2}{\partial y^2}\right)z \quad (1)$$

$$f(x,t) = (m + m_1)\frac{\partial^2 z}{\partial t^2} + 2(m + m_2)v\frac{\partial^2 z}{\partial t \partial x} + [(m + m_3)v^2 - T]\frac{\partial^2 z}{\partial x^2} \quad (2)$$

$$z_1 = (1/2)\sin\{(1 + v/c)\frac{\omega}{c}[c - v)t + x]\} - (1/2)\sin\{(1 - v/c)\frac{\omega}{c}[(c + v)t - x]\} \quad (4)$$

$$f_1 = \frac{c}{2L}\frac{1 - (1 + r_3)(v/c)^2}{\sqrt{1 + r_1 - [(1 + r_1)(1 + r_3) - (1 \pm r_2)^2](v/c)^2}} \quad (6)$$

$$(m + m_1)\frac{\partial^2 z}{\partial t^2} + 2m_2U\frac{\partial^2 z}{\partial t \partial x} + (m_3U^2 - T)\frac{\partial^2 z}{\partial x^2} = 0 \quad (18)$$

The subscripted m_1, m_2, and m_3 refer to the added mass due to the surrounding air, which is different for each term.

The terms involving bending stiffness D tend to be much smaller than the term involving tension T, but these may be needed to assure continuity in the cross-machine direction and to describe the behavior of slack edges (where T becomes very small). Excitation may enter as a deflection of a support (boundary condition), as a variation in the tension T (parametric excitation), or as a local aerodynamic force $f(x,y,t)$.

Threadline model

As a first small step, we can study the web equation for motions that are uniform across the entire web, neglecting any y-dependent variation in deflection z and tension T. We also neglect the bending stiffness terms since they are much smaller than the T term. These assumptions lead us to the equivalent of a "threadline," a thread string or chain being transported from one roll or spool to another.

We choose to solve this problem in a fixed coordinate system, so that we can later apply the end conditions, constituted by the support rolls, which are at fixed locations. A force balance on an infinitesimal length of such a moving thread leads to the partial differential equation:

See Equation 2

The first term on the right-hand side is mass times acceleration in our coordinate system, with the location x held constant. Since the web moves relative to this fixed coordinate system, Coriolis and centrifugal forces appear in the second and third terms. The third term also contains the restoring force due to tension T, which tends to bring the deflection z back to zero. If the velocity is too large or the tension too small, the restoring force disappears, and the threadline becomes unstable.

Please note that the T refers to the actual tension in the web; the apparent tension that one might deduce from the reaction forces on a roll supporting the thread or web is equal to $(T - mv^2)$ because the centrifugal force on the thread pulls away from the roll.

In the special case where $m_1 = m_2 = m_3 = 0$ (i.e., if the web is heavy and air loading effects are neglected), the first mode complementary solution of the equation is:

$$z_1 = \cos[2\pi f_1 t + (\pi x/L)(v/c)]\sin(\pi x/L) \quad (3)$$

where

L = length of the web span

which may be verified by obtaining the derivatives and inserting them back into Eq. 2. Another form of the same solution may be obtained by transforming it to traveling wave coordinates:

See Equation 4

where c^2 is defined as T/m and ω is the angular frequency. The natural frequency f_1 is:

$$f_1 = (c/2L)[1 - (v/c)^2] \quad (5)$$

The dependence of natural frequency on web speed is shown in **Fig. 1**. Note that the natural frequency decreases with increasing web velocity, showing the decrease in stability at high speeds. When $v = c$, the natural frequency goes to zero, the web "buckles," the solution for z diverges, and the web becomes unstable. The frequency at which this occurs is the "critical velocity."

A second special case is that in which $m_1 = m_2 = m_3$ (i.e., if all surrounding air moves with the air at velocity v and any boundaries restraining air motion are very far away). Exactly the same solution is obtained, except that $(m + m_1)$ must be substituted for m in the calculation of the actual wave velocity. The natural frequency f_1 and the critical velocity both drop proportionately; defining c as the phase speed of a wave on the web in a vacuum, $c = (T/m)^{1/2}$, the entire graph shrinks toward the origin.

In realistic cases, m_2 and m_3 tend to be smaller than m_1. When aerodynamic effects due to each term are analyzed separately, we find that an increase of m_1 reduces f_1 and causes the intercept at the ordinate to be depressed. An increase of m_3 reduces the critical velocity, causing the intercept at the abscissa to move toward the origin. The m_2 term acts in different ways depending on the

1. Natural frequency of a moving web for constant web tension ($m_1 = m_2 = m_3 = 0$)

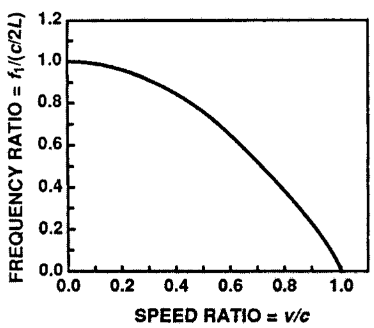

2. Effect of aerodynamic terms on the dynamics of the web

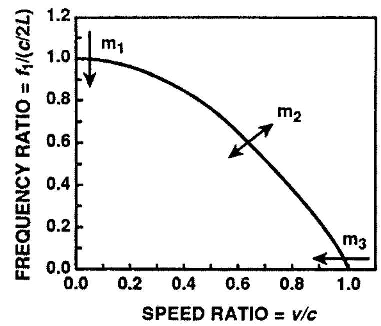

3. Effect of flow direction on the natural frequency of a running web ($r_1 = r_2 = r_3 = 1$)

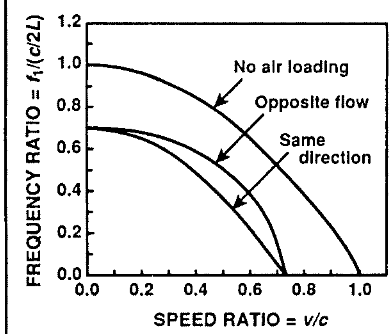

4. Added mass coefficient of a rectangular web

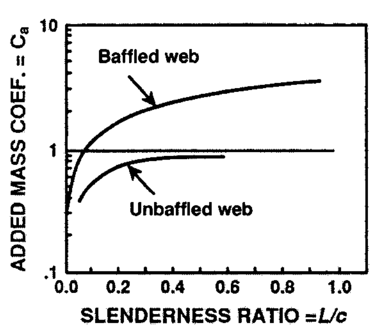

5. Geometry of the web and the enclosure

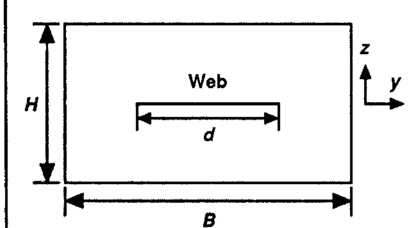

6. Added mass coefficient of a web in an enclosure

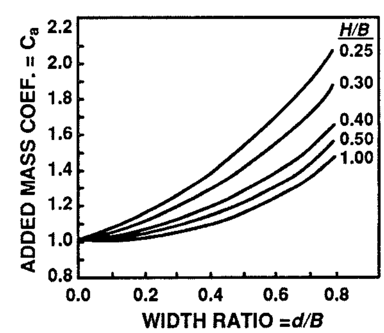

7. Speed distribution of the air flow example

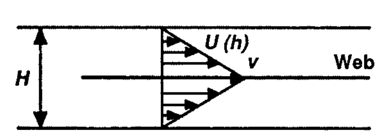

8. Fundamental frequency of the example web

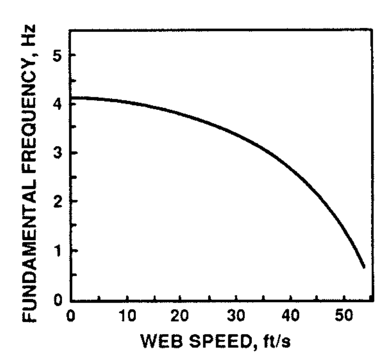

direction of flow. If the air flow near the web is in the same direction as the web motion, the curve shifts toward the origin. If the air is forced to flow counter to web motion, the curve will bulge out in the opposite direction, as shown in **Fig. 2**.

The fundamental frequency of a running web is (*6*):

See Equation 6

where

$r_1 = m_1/m$

$r_2 = m_2/m$

$r_3 = m_3/m$

The effect of flow direction appears in the sign of r_2. The positive sign of r_2 corresponds to the air flowing in the same direction as the web, while the negative sign is for contrary flow.

In the interesting special case where $m_1 = m_2 = m_3$, this frequency equation becomes

$$f_1 = \frac{c}{2L}\frac{1}{\sqrt{2}}\ [1 - 2(v/c)^2] \qquad (7)$$

for the same-directional flow, and

$$f_1 = \frac{c}{2L}\frac{1}{\sqrt{2}}\sqrt{1 - 2(v/c)^2} \qquad (8)$$

for the opposite flow. The natural frequency for the case of opposite flow is higher, as shown in **Fig. 3**, but the critical speed is the same for both cases.

Aerodynamic effects

Air loading due to transverse acceleration

The mass ($m + m_1$) is associated with the transverse acceleration of the web in the z direction. The equivalent mass (m_1), which the surrounding air adds to the mass of the web (m), can be obtained from the kinetic energy in the potential flow field generated by a z-direction displacement of the web. This depends on the mode shape of the deflection. Some special cases with well-known solutions are as follows.

1. If the span L is much longer than the web width d (the "slender body" case), the mid-span section undergoes almost uniform deflection, the air moves largely around the edges of the web (in the CD plane) rather than toward the ends of the span (in the MD plane), and the added mass per unit area of the web due to the potential flow field becomes:

$$m_1 = (\pi/4)\rho d \qquad (9)$$

where

ρ = air density

d = width of web.

2. If the web shows transverse ripples at a higher mode, with a wavelength λ much shorter than the width of the web d, the air moves largely from peak to trough, and the added mass is only:

$$m_1 = (\rho\lambda)/\pi \qquad (1$$

3. For comparison, the added mass of an unbaffled rectangular sheet (that is, having free edges all around) moving as a unit is

$$m_1 = \frac{\pi}{4}\rho d \frac{1}{\sqrt{1 + 1/s^2}} \left(1 - \frac{0.425\, s}{1 + s^2}\right) \qquad (11)$$

where s is the slenderness ratio L/d, and $L > d$.

4. On the other hand, the added mass of a baffled rectangular sheet (i.e., surrounded by a fixed plate in the same plane) moving as a unit is

$$m_1 = 0.96\rho\, ds^{1/2} \qquad (12)$$

where $s = L/d$, which must be neither very large nor very small.

These limiting cases give us an indication of the magnitude of m_1. If neither Eq. 9 or Eq. 10 can be applied, the added mass of a web should be between the values given by Eqs. 11 and 12, since the ends are baffled while the edges are free. Equations 11 and 12 are compared in **Fig. 4**, where the added mass coefficient C_a is defined by

$$m_1 = C_a\,(\pi/4)\rho d \qquad (13)$$

When a web is surrounded by an enclosure, the aerodynamic terms change. The term m_1 for a narrow and long web in an enclosure can be calculated by assuming potential flow in the CD plane, obtaining the stream function by Southwell's Relaxation Method [a finite difference method (7)], summing up the kinetic energy in the flow field, and referring it to the web velocity. We carried out sample computations for the simple geometry shown in **Fig. 5**.

For each set of values of H (height) and B (width of enclosure), only a quarter of the enclosed air needed to be computed because of symmetry. That quarter was divided into thousands of square cells. The governing equation of two-dimensional motion in an incompressible, inviscid fluid is that the Laplacian of either the potential function or the stream function ψ is equal to zero. This equation can be changed to a simple finite difference equation, which states that the value of the stream function at any point is equal to the average of the values at the adjacent points.

Boundary conditions used were unit velocity at the web ($\partial\psi/\partial y = 1$), parallel flow at the wall (ψ = constant), and zero horizontal velocity in the plane of the web ($\partial\psi/\partial z = 0$). From the resulting stream function, the velocity components in each cell were then calculated relative to the unit vertical velocity of the web, and the total kinetic energy in the flow field was summed. Since the nominal velocity of the web was taken as unity, the added mass was obtained by setting this kinetic energy equal to 1/2 m_1. The results are shown in **Fig. 6**. As expected from Eq. 9, C_a approaches 1.0 when the height and width of the enclosure are much larger than the web width. For smaller enclosures, both width and height affect C_a significantly.

Air loading due to Coriolis acceleration

The mass m_2 is associated with the Coriolis force. The effect of the surrounding air depends not only on the amount of air moving but also on whether it moves with the web or against it. If it moves with the web, the air adds to the mass; if it moves opposite the web motion, it reduces the effective mass. Two limiting cases are:

1. If the web is slender ($L >> d$) and all the air moves with the web, then the added mass is the same as m_2 in Eq. 9.

2. If the surrounding air is stationary except for a thin boundary layer, the effective mass can be calculated from the integral of the velocity through both upper and lower boundary layer thicknesses δ:

$$m_2 = \rho(\delta_U^* + \delta_L^*) \qquad (14)$$

where

U = air speed

δ^* = displacement thickness.

The displacement thickness δ^* is defined as

$$\delta^* = \left| (1/v)\int_0^{\delta} U(h)\, dh \right| \qquad (15)$$

where

v = running speed of the web

$U(h)$ = flow speed.

Air loading due to centripetal acceleration

The mass m_3 is associated with the centrifugal force due to curvature of the moving web. The effect of the surrounding air depends on the amount of air moving with the web. Two limiting cases are:

1. If the web is slender ($L >> d$) and all the air around the web moves with it, the added mass is again the same as m_1 in Eq. 9.

2. If the flow field of surrounding air is stationary and the boundary layer of air moving with the web is relatively thin, the added mass can be calculated from the integral of the

9. Experimental setup

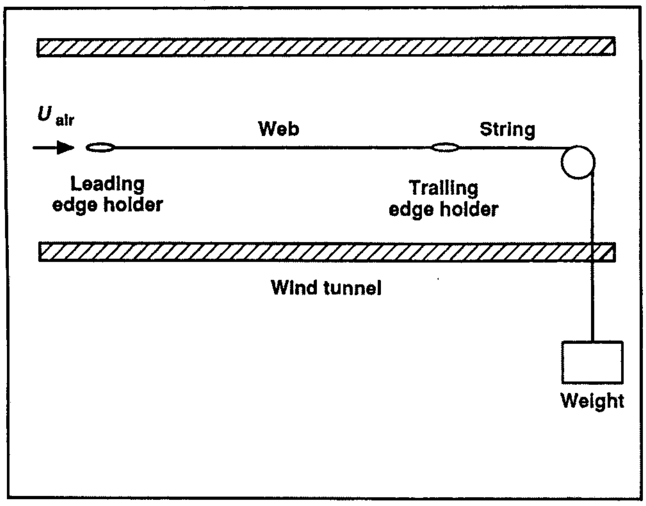

10. Typical shapes of an unstable web in a wind

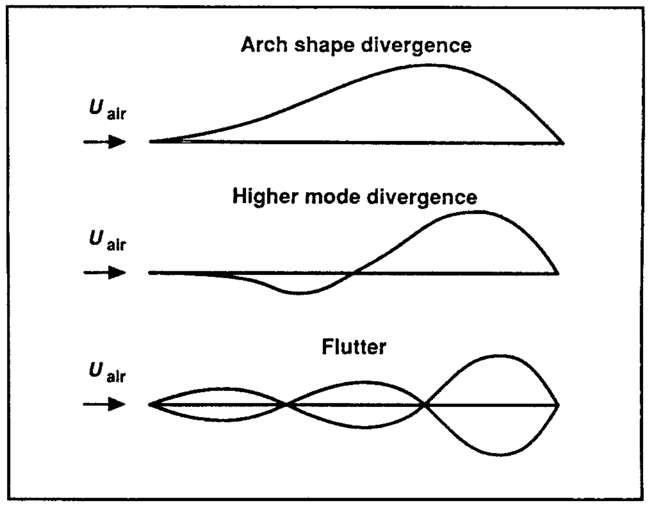

11. Static stability boundary of a stationary web in a wind

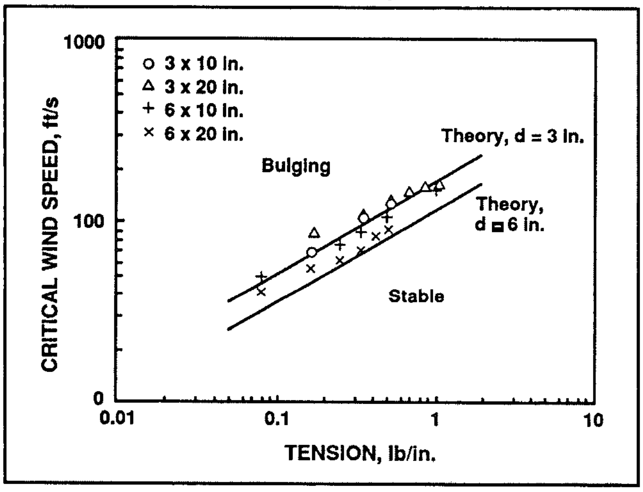

12. Dynamic stability boundary of a stationary web in a wind

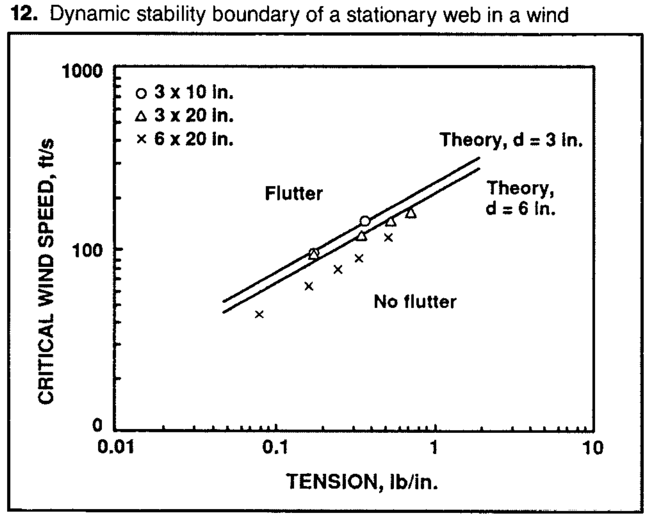

square of the velocity of the air $U(h)$ through both boundary layer thicknesses:

$$m_3 = \pi(\theta_U + \theta_L) \qquad (16)$$

where θ is the momentum thickness defined as

$$\theta = (1/v^2)\int_0^{\delta} U^2(h)\, dh \qquad (17)$$

Note that the equations for boundary layer growth on a flat plate are not applicable to a moving web, since the leading-edge condition is completely different. New calculations and measurements are required.

Example calculation

Consider a simple flow distribution in an enclosure as shown in **Fig. 7**, with

H = 1 ft

B = 2 ft 6 in.

d = 2 ft

L = 3 ft

m = 0.0155 lb/ft^2

π = 0.0765 lb/ft^3

T = 4 lb/ft

Then

H/B = 0.4

d/B = 0.8

C_a = 1.66 from Fig. 6

δ^* = $H/4$ from Eq. 15

θ = $H/6$ from Eq. 17

c = $(T/m)^{1/2}$ = 91.1 ft/s

The aerodynamic masses are

$$m_1 = (1.66\pi/4)\rho d = 0.199 \text{ lb/ft}^2$$

for $r_1 = 12.8$

$$m_2 = 2\rho\delta^* = (1/2)\rho H = 0.0383 \text{ lb/ft}^2$$

for $r_2 = 2.47$

$$m_3 = 2\rho\theta = (1/3)\rho H = 0.0255 \text{ lb/ft}^2$$

for $r_3 = 1.65$.

Then, from Eq. 6, the fundamental natural frequency of the running web becomes

$$f_1 = 15.2(1 - 0.000319v^2)/(13.8 - 0.00367v^2)^{1/2}$$

where f_1 is in Hz and v is in ft/s. The fundamental frequency of the example web is shown in **Fig. 8** as a function of web speed.

Wind tunnel tests

Wind tunnel tests have been conducted to verify the interaction between the web and the surrounding air, beginning with the simple case of slender webs. For support-to-support air velocities (machine direction), the governing equation of a stationary slender web surrounded by flowing air with a negligible boundary layer is:

See Equation 18

where

$$m_1 = m_2 = m_3 = (\pi/4)\rho d \qquad (19)$$

From a simplified analysis (*6*), two different critical conditions are expected:

$$U_{div} = \sqrt{\frac{4T}{\pi \rho d}} \qquad (20)$$

$$U_{flt} = \sqrt{\frac{T}{m}}\sqrt{1 + \frac{4m}{\pi \rho d}} \qquad (21)$$

where

U_{div} = critical air speed for static instability (divergence)

U_{flt} = critical air speed for dynamic instability (flutter).

U_{div} in Eq. 20 is the critical wind speed above which the web begins to bulge or "sail" upward or downward (static divergence), and Eq. 21 gives the critical condition for violent oscillations (flutter). Note that U_{flt} is always higher than U_{div}. Though U_{flt} is affected by the web mass m, U_{div} is independent of m. These instabilities were tested by experiment.

Test setup

Rectangular thin papers were tested in a subsonic wind tunnel. The test section is 24.5 in. wide and 16.25 in. high. Tested papers have dimensions of 3 in. × 10 in., 3 in. × 20 in., 6 in. × 10 in., and 6 in. × 20 in. For those dimensions, H/B = 0.673 and $d/B \leq$ 0.245. Thus C_a = 1.0 from Fig. 6. The flow speed is uniform across the test section. Therefore, the tested papers can be considered as webs in an infinite, uniform flow field.

The leading and trailing edges are restrained from vertical motion, while the other two edges are free to move. Tension is applied through the trailing edge, as shown in **Fig. 9**. The test variables are (a) the width and length of the web, (b) tension, and (c) air velocity.

Test results

Both static divergence (steady deflection of the web) and dynamic instability (flutter of the web) were observed. As the wind speed is increased from zero, the paper starts to diverge at a critical wind speed. It bulges out either upward or downward. If the wind speed is increased further, then the displacement is also increased, and in some cases a higher mode (multiple-wave) divergence occurs. If the speed is increased even more, a traveling wave having very low speed occurs. The oscillation frequency and amplitude grow with the wind speed into a pronounced flutter, which becomes very violent at higher wind speed. Critical speed of dynamic instability is always higher than that of static instability, as expected from theory. Some typical shapes of a web during instability are shown in **Fig. 10**. In some cases, static divergence is suddenly changed to flutter by an increase in wind speed, while in other cases there is a stable range between static and dynamic instability regions.

Critical wind speeds of static instability and flutter were determined for each set of test conditions, for given dimensions of the paper and tension. **Figure 11** shows the stability boundaries of static divergence. Compared theoretical curves are from Eq. 20. The experimental results are higher than the theoretically expected critical wind speeds. For the critical conditions of flutter, the experimental results are lower than the theoretical curves, as shown in **Fig. 12**, where the curves are from Eq. 21.

Summary and conclusions

The successful application of the traveling threadline model of a running web depends on the correct application of three different aerodynamic terms, which are related to transverse, Coriolis, and centripetal accelerations. The effect of these terms has been obtained for a number of cases. This makes it possible to calculate natural frequencies for particular web motions. These frequencies are an indication of stability; when a frequency goes to zero, the web becomes unstable.

The example of MD flows showed that air-web interaction plays an essential role in web instability. Wind tunnel tests were done for narrow and long webs, and the test results were compared with theory. Both steady deflection and flutter were observed. The experimental results have the same trends as indicated by the slender-body theory, but the experimental critical wind speeds for static divergence are higher than the theoretical values, while the experimental values for flutter fall below the theoretical curves. Except for these small discrepancies, the slender-body model appears to represent the physics of the instability of a slender web correctly. Therefore, this approach seems to be well suited to long-span web motions, such as occur in drying ovens.

Expansions of the work to edge flutter in the presence of lateral (cross-direction) air flow, such as occurs in paper machines, is in progress, with a forced vibration technique being used in the wind tunnel. Verification with air flows on running webs is planned for the long term.□

Literature cited

1. Pramila, A., Tappi J. 69(7): 70(1986).
2. Pramila, A., J. Sound and Vibration 113(1): 198(1987).
3. Race, E., Wheeldon, J. B., and Fraser-Clark, D., Tappi 51(7): 51A(1968).
4. Soininen, M. A., Air flow phenomena in a multicylinder dryer with drying screens, Papper och Tra 52(Special-nummer 4a): 187(1970).
5. Mujumdar, A. S., Sheet flutter in high-speed paper dryers, IPPTA (Indian Pulp and Paper Technical Association) 11(2): 93(1974) (April, May, and June).
6. Chang, Y. B., An experimental and analytical study of web flutter, Ph.D. dissertation, Oklahoma State University, December 1990.
7. Chow, C. Y., An Introduction to Computational Fluid Mechanics, Wiley, New York, 1979.

The computations and experiments reported were made possible by the support of the Web Handling Research Center at Oklahoma State University.

Received for review May 31, 1990.

Accepted Oct. 9, 1990.

Presented at the TAPPI 1990 Engineering Conference.